

## PAPER

# SGAC: A Graph Neural Network Framework for Imbalanced and Structure-Aware AMP Classification

Yingxu Wang,<sup>1</sup> Victor Liang,<sup>2</sup> Nan Yin,<sup>3</sup> Siwei Liu<sup>\*2</sup> and Eran Segal<sup>\*1,4</sup>

<sup>1</sup>Department of Machine Learning, Mohamed bin Zayed University of Artificial Intelligence, AI Diyah St, 7909, Abu Dhabi, United Arab Emirates, <sup>2</sup>School of Natural & Computing Science, University of Aberdeen, 32 Elphinstone Rd, AB24 3EU, Scotland, United Kingdom,

<sup>3</sup>Department of Computer Science and Engineering, Hong Kong University of Science and Technology, Hong Kong, China and

<sup>4</sup>Department of Molecular Cell Biology, Weizmann Institute of Science, Rehovot, Israel

\*Corresponding author. siwei.liu@abdn.ac.uk, Eran.Segal@weizmann.ac.il

FOR PUBLISHER ONLY Received on Date Month Year; revised on Date Month Year; accepted on Date Month Year

## Abstract

Classifying Antimicrobial Peptides (AMPs) from the vast collection of peptides derived from metagenomic sequencing offers a promising avenue for combating antibiotic resistance. However, most existing AMP classification methods rely primarily on sequence-based representations and fail to capture the spatial structural information critical for accurate identification. Although recent graph-based approaches attempt to incorporate structural information, they typically construct residue- or atom-level graphs that introduce redundant atomic details and increase structural complexity. Furthermore, the class imbalance between the small number of known AMPs and the abundant non-AMPs significantly hinders predictive performance. To address these challenges, we employ lightweight OmegaFold to predict the three-dimensional structures of peptides and construct peptide graphs using  $C_\alpha$  atoms to capture their backbone geometry and spatial topology. Building on this representation, we propose the **Spatial GNN-based AMP Classifier (SGAC)**, a novel framework that leverages Graph Neural Networks (GNNs) to extract structural features and generate discriminative graph representations. To handle class imbalance, SGAC incorporates Weight-enhanced Contrastive Learning to cluster structurally similar peptides and separate dissimilar ones through adaptive weighting, and applies Weight-enhanced Pseudo-label Distillation to generate high-confidence pseudo labels for unlabeled samples, achieving balanced and consistent representation learning. Experiments on publicly available AMP and non-AMP datasets demonstrate that SGAC significantly achieves state-of-the-art performance compared to baselines.

**Key words:** Amp prediction, Graph Neural Networks

## 1. Introduction

The increasing prevalence of antibiotic resistance [37, 45] has intensified the demand for new antimicrobial drugs. Antimicrobial peptides (AMPs), which are short peptides with broad-spectrum antimicrobial activity, are predominantly 10 to 50 amino acids in length as reported in public databases. AMPs are regarded as successors that can “surpass their predecessors” due to their unique antimicrobial mechanisms and broad-spectrum activity [35, 44, 57, 6]. In recent years, advanced computational methods such as artificial intelligence and molecular simulation have been extensively applied in the field of AMP development, offering new opportunities for the research and development of these novel antimicrobial molecules [34, 24, 42].

During the evolutionary process of microorganisms, they engage in mutual competition, leading to the production of numerous substances that can resist other microorganisms. The genetic fragments of microorganisms contain many potential sequences that could be encoded as antimicrobial peptides,

forming a rich reservoir of antimicrobial peptide sources [4, 41]. Numerous studies have utilized metagenomic sequencing to mine potential antimicrobial peptides [59, 29, 13]: beginning with the collection of metagenomic sequencing data from diverse sources to identify open reading frames (ORFs) [12] within these sequences—those that have the potential to encode proteins. Following this, classifiers are trained using historical data of AMPs and non-AMPs to learn the patterns characteristic of AMPs. Subsequently, these well-trained classifiers are employed to sort through the open reading frames and categorize the potential AMPs. For example, Ma et al. [34] integrated multiple models, including LSTM [62] and BERT [14], to construct an AMP mining pipeline. From 154,723 metagenomic sequencing data, they identified 2,349 potential AMPs and synthesized 216 of them, with 181 exhibiting antimicrobial activity. Similarly, Torres et al. [42] used MetaProdigal [25], CD-Hit [19], and SmORFinder [16] to screen 1,773 human gut metagenomes, identifying 444,054 potential peptides, and predicted their antimicrobial activity using models such as random forests [3] and BERT, ultimately

determining 323 candidate AMPs. They selected 78 of these for synthesis and in vitro experiments, which confirmed that 55 exhibited antimicrobial activity. Compared to the previous two studies, Santos-Jnior et al. [39] utilized a larger dataset, leveraging 63,410 public metagenomes and 87,920 high-quality prokaryotic genomes. Initially, they employed the MetaProdigal [25] tool to predict all ORFs within the metagenomes. Following this, they used the CD-Hit [19] tool to cluster the predicted smORFs, identifying non-redundant peptide sequence families. Finally, they applied the Macrel tool [38], a random forest-based machine learning pipeline, to predict potential antimicrobial peptides from large peptide datasets, resulting in 863,498 non-redundant candidate antimicrobial peptides. They selected 100 of these for synthesis and in vitro experiments, which confirmed that 79 exhibited antimicrobial activity.

Previous research has shown that identifying effective AMPs is a complex process that involves both computational screening and resource-intensive in vitro validation [32, 55, 1]. To reduce this experimental burden, earlier studies have primarily relied on sequence-based models such as LSTM [34] and Random Forest [39] to discover distinguish AMPs and non-AMPs. Although these methods achieve moderate success, they fail to capture the essential spatial organization and geometric dependencies underlying peptide bioactivity. Recent advances in graph-based learning methods typically utilize pretrained protein language models (PLMs) such as AlphaFold2 [27] and ESMFold [44] to predict the 3D spatial structures of peptides and then construct graphs based on residue- or all-atom-level representations [36, 18, 40]. However, when applied to large-scale peptide datasets, this pipeline incurs extremely high preprocessing costs for structure prediction and graph construction [21, 7]. In addition, the constructed graphs are typically dense and contain redundant atomic details, which increase structural complexity and substantially raise the computational burden of downstream graph representation learning [58, 61, 17]. Beyond the architectural limitations of existing models, a fundamental challenge in AMP prediction arises from the severe class imbalance inherent in available datasets, where AMPs constitute only a small fraction of the overall peptide population [9, 10]. This imbalance tends to bias the learning process toward the dominant non-AMP class, limiting the model's ability to generalize to rare yet biologically important samples. As a result, existing methods often exhibit reduced discriminative power and unstable performance when applied to large-scale or real-world peptide applications.

To address the limitations of existing methods, we first predict the 3D spatial structure of each peptide using a lightweight pretrained protein language model, OmegaFold [54]. From the predicted structures, we construct peptide graphs using  $C_\alpha$  atoms to capture backbone geometry and spatial topology for accurate AMP classification. Then, we propose a novel framework, SGAC, which employs a Graph Neural Network (GNN) as the backbone encoder to learn spatial characteristics and generate discriminative graph representations for each peptide graph. To enhance representation learning under class imbalance, SGAC introduces two complementary modules: Weight-enhanced Contrastive Learning and Weight-enhanced Pseudo-label Learning. The contrastive module assigns adaptive weights to peptide pairs, improving the model's ability to distinguish positive and negative samples by clustering structurally similar peptides and separating dissimilar ones, thereby strengthening AMP-specific structural discrimination. The pseudo-label module

incorporates weight-aware optimization to generate high-confidence pseudo labels for unlabeled peptides, ensuring semantic consistency between labeled and unlabeled data while refining the representation of minority AMP samples.

The contributions of our paper can be summarized as follows:

- We propose a lightweight peptide graph construction mechanism for spatial AMP prediction, which predicts 3D structures using OmegaFold and constructs graphs based on  $C_\alpha$  atoms, effectively capturing backbone geometry while minimizing redundant atomic details.
- We develop SGAC, which employs GNNs to encode spatial characteristics of each peptide and integrates Weight-enhanced Contrastive Learning and Pseudo-label Distillation to address the class imbalance and improve classification accuracy.
- Experiments on publicly available AMP and non-AMP datasets demonstrate that our SGAC significantly outperforms traditional sequence-based methods and achieves state-of-the-art performance, validating its effectiveness in AMP classification.

## 2. Methodology

In this paper, we focus on improving the prediction accuracy of AMPs and non-AMPs by leveraging the spatial structural information of peptides. We first predict the 3D structures of peptides based on their amino acid sequences using OmegaFold [54] and construct peptide graphs from the  $C_\alpha$  positions of the residues [61, 31, 53]. Then, we introduce a novel approach, SGAC, which leverages a Graph Neural Network (GNN) as a **Graph Encoder** to generate comprehensive peptide representations. To address the class imbalance issue and refine predictions, **Weight-enhanced Contrastive Learning** clusters similar peptides and separates dissimilar ones by assigning specific weights to positive and negative pairs. Furthermore, **Weight-enhanced Pseudo-label Distillation** dynamically generates reliable and high confidence pseudo labels, ensuring balanced representation of AMPs and non-AMPs while enforcing consistency. The overview of the above process is shown in Figure 1.

### 2.1 Graph Construction

Let  $P = \{a_1, a_2, \dots, a_n\}$  represents a peptide sequence consisting of  $n$  amino acids. The AMP and non-AMP data are initially provided as primary amino acid sequences without atomic-level structural details. To address this limitation, we utilize OmegaFold [54], a pre-trained protein language model that can infer the three-dimensional spatial coordinates of each residue from its amino acid sequence. By leveraging both AMP and non-AMP data by OmegaFold, we obtain the corresponding 3D spatial structures for each amino acid residue  $a_i$ . To focus on structural analysis, we only extract the positions of the  $C_\alpha$  atoms, which serve as representative spatial coordinates for the amino acid backbone. Such a process will generate a set of 3D coordinates denoted as  $\mathbf{R} = \{\mathbf{r}_1, \mathbf{r}_2, \dots, \mathbf{r}_n\} \in \mathbb{R}^{N \times 3}$ , where  $\mathbf{r}_i \in \mathbb{R}^3$  corresponds to the spatial position of the  $C_\alpha$  atom for amino acid  $a_i$ .

To represent the peptides as graphs, we use an undirected graph  $G = (V, E, \mathbf{X})$  to represent each peptide, where  $V$  denotes the set of nodes,  $E$  the set of edges, and  $\mathbf{X}$  the node feature matrix. The nodes  $V$  correspond to the  $C_\alpha$  atoms of the

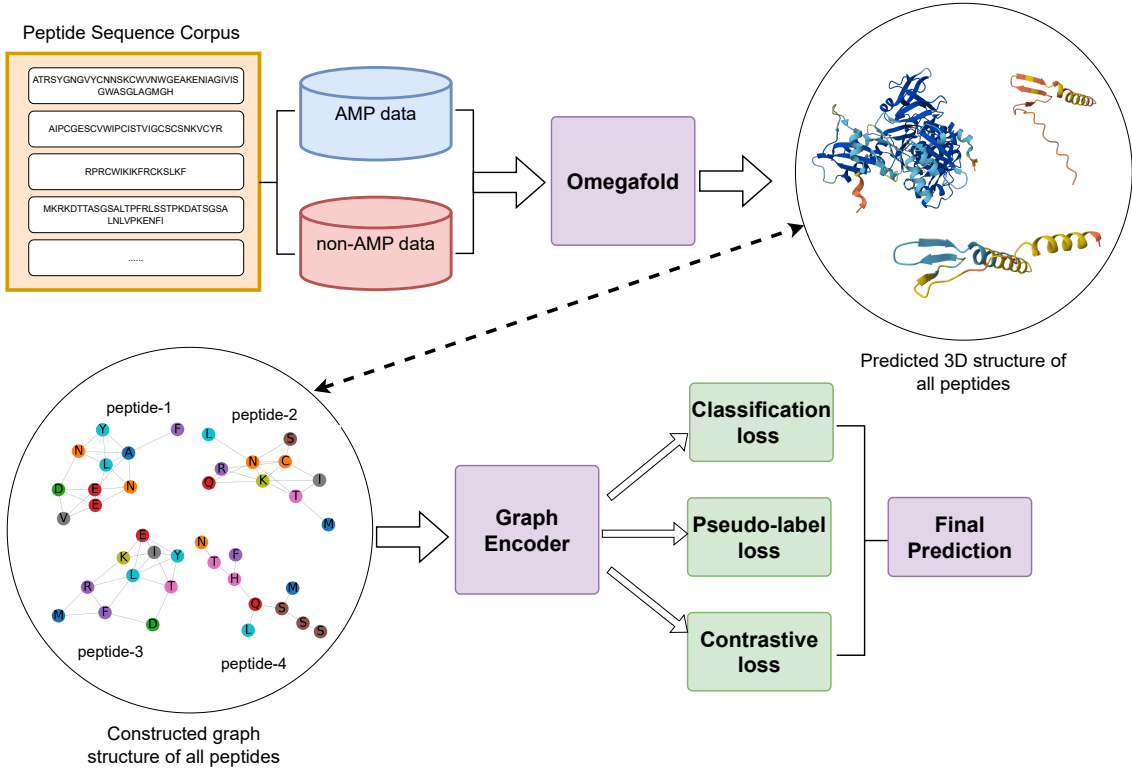


**Fig. 1.** Overall framework of our SGAC model. The framework consists of multiple stages designed to enhance AMP classification. Initially, Omegafold is employed to predict the three-dimensional (3D) structure of peptides based on their amino acid sequences, generating peptide graphs where nodes represent  $C_\alpha$  atoms. These graphs are then processed by a Graph Neural Network (GNN) encoder to capture structural and relational features. Then, the embeddings produced by Graph Encoder are refined using three key components: Weight-enhanced Contrastive Learning, which improves feature separation between AMPs and non-AMPs; Weight-enhanced Pseudo-label Distillation, which dynamically refines predictions using high-confidence pseudo labels; and a Classification Loss, which ensures accurate supervised learning by directly optimizing the classification performance. Finally, our SGAC model produce the final prediction results.

amino acids, defined as  $V = \{v_1, v_2, \dots, v_n\}$ , with each node  $v_i$  representing the  $C_\alpha$  atom of amino acid  $a_i$ . Edges in the graph are determined based on the Euclidean distances between  $C_\alpha$  atoms. Specifically, an edge is established between nodes  $v_i$  and  $v_j$  if the distance between their corresponding  $C_\alpha$  atoms is less than a predefined threshold  $\delta$ :

$$E = \{(v_i, v_j) \mid \|\mathbf{r}_i - \mathbf{r}_j\|_2 < \delta, i \neq j\}, \quad (1)$$

where  $\delta$  controls the connectivity of the graph. The node feature matrix  $\mathbf{X}$  encodes the biochemical identity of each amino acid. We produce a comprehensive set of unique amino acid types from the AMP and non-AMP datasets to generate these features. Each amino acid is then represented as a one-hot encoded vector based on its sequence identity, ensuring that the feature matrix  $\mathbf{X}$  captures essential sequence-based information.

The constructed graph  $G$  captures the spatial relationships between amino acids within the peptide, providing a robust framework for analysing protein structure and function. Additionally, the focus on spatial connectivity through the  $C_\alpha$  atoms ensures that the graph  $G$  captures essential structural features of each peptide, which are critical for distinguishing AMPs from non-AMPs.

## 2.2 Graph Encoder

Peptides are intricate biomolecules whose functions are deeply influenced by their structure and spatial relationships. To accurately distinguish AMPs from non-AMPs, we transform the input peptide graphs into graph representations to capture essential structural and relational information within peptides. This approach leverages peptides' intricate spatial patterns and connectivity to enhance predictive accuracy and biological relevance.

Given a peptide graph  $G = (V, E, \mathbf{X})$ , we leverage a Graph Neural Network (GNN) to encode its structure and node attributes. Let  $\mathbf{h}_v^{(l)}$  represent the embedding for node  $v$  at the  $l$  th layer of the network. The initial embedding  $\mathbf{h}_v^{(0)}$  is defined by  $\mathbf{h}_v^{(0)} = \text{MLP}(\mathbf{x}_v)$ , where the  $\text{MLP}(\cdot)$  is a learnable multi-layer perceptron that maps the node feature  $\mathbf{x}_v$  into the latent space. Subsequently, for each node  $v \in V$ , the embedding  $\mathbf{h}_v^{(l)}$  is updated iteratively through a message-passing framework. At each iteration, the embedding of  $v$  is updated by aggregating information from its neighboring nodes  $\mathcal{N}(v)$  from the previous layer, and this aggregated information is combined with the embedding of  $v$  from the same layer. Formally, this update process is defined as:

$$\mathbf{h}_v^l = \mathcal{C}^{(l-1)} \left( \mathbf{h}_v^{l-1}, \mathcal{A}^{(l-1)} \left( \left\{ \mathbf{h}_u^{l-1} \right\}_{u \in \mathcal{N}(v)} \right) \right), \quad (2)$$

where  $\mathcal{A}^{(l-1)}$  denotes the aggregation operation at the  $l-1$ -th layer, which aggregates embeddings from the neighbors of  $v$ , and  $\mathcal{C}^{(l-1)}$  represents the combination operation at the  $l-1$ -th layer, which integrates the aggregated neighbor information with the embedding of  $v$  itself. This iterative message-passing mechanism enables the GNN to effectively capture both the local structural interactions among amino acids and the global topology of the peptide graph.

After  $L$  layers of iterative updates, a graph-level representation  $\mathbf{z}$  is computed for each peptide graph  $G$  using a readout function, which aggregates the node representations at the final layer:

$$\mathbf{z} = F(G) = \text{READOUT} \left( \left\{ \mathbf{h}_v^L \right\}_{v \in \mathcal{V}} \right), \quad (3)$$

where  $\mathbf{z}$  is the graph-level representation for each peptide generated by the GNN function  $F(\cdot)$ . The READOUT function can be implemented in various strategies, such as summation, averaging, maximization of node embeddings [56, 51, 60] or incorporating a virtual node [30, 52, 49] to capture global graph information. The graph-level representation  $\mathbf{z}$  captures the peptide's structural and relational characteristics, providing a robust foundation for distinguishing AMPs from non-AMPs.

### 2.3 Weight-enhanced Contrastive Learning

Contrastive learning enhances the discriminative power of feature representations by aligning labeled similar samples while ensuring separation from dissimilar ones [8, 46], which is effective for distinguishing AMPs from non-AMPs by capturing their unique structural and relational differences. However, a critical challenge in AMP classification lies in the class imbalance, where non-AMP samples significantly outnumber AMP samples. This imbalance can lead standard contrastive learning methods to overemphasize the majority class (non-AMPs), thereby degrading the model's ability to classify the minority class (AMPs) accurately.

To address this issue, we introduce Weight-enhanced Contrastive Learning, a tailored approach that incorporates class-specific weights to balance the influence of positive and negative samples during training. By appropriately weighting contributions from each class, this method mitigates the effects of class imbalance, ensuring that the learned representations reflect the distinguishing features of AMPs while maintaining robust discrimination against non-AMPs.

Assuming the Graph Encoder has  $L$  message passing layers, we first extract the graph embeddings of the  $L$ -th layer, where  $\mathbf{Z}^L = [\mathbf{z}_1^L, \mathbf{z}_2^L, \dots, \mathbf{z}_{|\mathcal{N}_{\text{label}}|}^L]^T \in \mathbb{R}^{|\mathcal{N}_{\text{label}}| \times d}$  for  $|\mathcal{N}_{\text{label}}|$  labeled peptide graphs, where  $\mathbf{z}_i^L \in \mathbb{R}^d$  is the  $d$ -dimensional embedding of the  $i$ -th labeled peptide, and the corresponding label vector  $\mathbf{y} = [y_1, y_2, \dots, y_{|\mathcal{N}_{\text{label}}|}]$ . Contrastive learning aims to optimize embeddings such that peptides sharing the same label are positioned closer together in the latent space. In contrast, those with different labels are pushed further apart. To achieve this, the pairwise Euclidean distance between embeddings is computed as:

$$D_{ij} = \left\| \mathbf{z}_i^L - \mathbf{z}_j^L \right\|_2, \quad \forall i, j \in \{1, 2, \dots, |\mathcal{N}_{\text{label}}|\}. \quad (4)$$

To address the issue of class imbalance, we incorporate class-specific weights, denoted as  $\omega_{cl}^{\text{pos}}$  for positive pairs (samples with the same label) and  $\omega_{cl}^{\text{neg}}$  for negative pairs (samples with different labels). Specifically,  $\omega_{cl}^{\text{pos}}$  is calculated as:

$$\omega_{cl}^{\text{pos}} = 1 - \frac{|\mathcal{N}_{\text{label}}^{\text{pos}}|}{|\mathcal{N}_{\text{label}}^{\text{pos}}| + |\mathcal{N}_{\text{label}}^{\text{neg}}|}, \quad (5)$$

while  $\omega_{cl}^{\text{neg}}$  is calculated by:

$$\omega_{cl}^{\text{neg}} = 1 - \frac{|\mathcal{N}_{\text{label}}^{\text{neg}}|}{|\mathcal{N}_{\text{label}}^{\text{pos}}| + |\mathcal{N}_{\text{label}}^{\text{neg}}|}, \quad (6)$$

where  $\mathcal{N}_{\text{label}} = \mathcal{N}_{\text{label}}^{\text{pos}} + \mathcal{N}_{\text{label}}^{\text{neg}}$ ,  $\mathcal{N}_{\text{label}}^{\text{pos}}$  and  $\mathcal{N}_{\text{label}}^{\text{neg}}$  denote the sets of AMP and non-AMP samples in the labeled dataset, respectively, and  $|\mathcal{N}_{\text{label}}^{\text{pos}}|$  and  $|\mathcal{N}_{\text{label}}^{\text{neg}}|$  represent their respective sizes.

These weights ensure that both classes contribute proportionally to the learning process. The positive contrastive loss, which encourages embeddings of peptides with the same label to cluster together, is defined as:

$$\mathcal{L}_{cl}^{\text{pos}} = \omega_{cl}^{\text{pos}} \sum_{i=1}^{|\mathcal{N}_{\text{label}}|} \sum_{j=1}^{|\mathcal{N}_{\text{label}}|} \mathbb{I}(y_i = y_j) D_{ij}^2, \quad (7)$$

$$\forall i, j \in \{1, 2, \dots, |\mathcal{N}_{\text{label}}|\},$$

where  $\mathbb{I}(\cdot)$  is an indicator function that equals 1 if  $y_i = y_j$ , and 0 otherwise. This formulation allows for the effective integration of class-specific contributions, improving the model's ability to capture the intrinsic relationships within the peptide data, even when the class distribution is imbalanced.

To ensure sufficient separation between embeddings of peptides with different labels, we apply a margin  $m$  for negative pairs. This margin enforces a minimum distance between dissimilar samples, thereby enhancing the discriminative power of the model. The negative contrastive loss is defined as:

$$\mathcal{L}_{cl}^{\text{neg}} = \omega_{cl}^{\text{neg}} \sum_{i=1}^{|\mathcal{N}_{\text{label}}|} \sum_{j=1}^{|\mathcal{N}_{\text{label}}|} \mathbb{I}(y_i \neq y_j) \max(0, m - D_{ij})^2, \quad (8)$$

$$\forall i, j \in \{1, 2, \dots, |\mathcal{N}_{\text{label}}|\},$$

where  $\mathbb{I}(y_i \neq y_j)$  is an indicator function that equals 1 if  $y_i \neq y_j$  and 0 otherwise. The term  $\max(0, m - D_{ij})$  ensures that negative pairs contribute to the loss only when their distance  $D_{ij}$  is less than the margin  $m$ .

Finally, the overall Weight-enhanced Contrastive Loss,  $\mathcal{L}_{cl}$ , combines the positive and negative losses, normalized by the total number of sample pairs to account for the dataset size, which is defined as follows:

$$\mathcal{L}_{cl} = \frac{1}{|\mathcal{N}_{\text{label}}| * (|\mathcal{N}_{\text{label}}| - 1)} (\mathcal{L}_{cl}^{\text{pos}} + \mathcal{L}_{cl}^{\text{neg}}). \quad (9)$$

This formulation ensures a balanced optimization of embeddings, effectively leveraging both positive and negative pairs while mitigating the effects of class imbalance.

### 2.4 Weight-enhanced Pseudo Label Distillation

Pseudo-label learning leverages unlabeled data by assigning high-confidence pseudo-labels to enable iterative refinement of the model's understanding of the data distribution [50]. This process ensures semantic consistency across different latent spaces and is particularly useful for addressing the scarcity of labeled AMP data while facilitating the discovery of novel AMP sequences. However, traditional pseudo-label distillation methods often suffer from the inherent class imbalance between AMP and non-AMP samples, resulting in model bias toward the majority class.

To address this issue, we propose Weight-Enhanced Pseudo-Label Distillation, a method designed to dynamically balance the contributions of AMP and non-AMP samples while aligning semantic information between labeled and unlabeled data. Additionally, this method incorporates soft-label refinement to produce accurate peptide representations, effectively mitigating the impact of class imbalance.

Assuming the Graph Encoder consists of  $L$  message-passing layers, we produce pseudo-labels for unlabeled peptides using the embeddings generated from the  $l$ -th hidden layer. These embeddings are represented as  $\mathbf{Z}^l = [\mathbf{z}_1^l, \mathbf{z}_2^l, \dots, \mathbf{z}_{|\mathcal{N}_{\text{unlabel}}|}^l]^T \in \mathbb{R}^{|\mathcal{N}_{\text{unlabel}}| \times d}$ , where  $|\mathcal{N}_{\text{unlabel}}|$  denotes the number of unlabeled peptide graphs, and  $\mathbf{z}_i^l \in \mathbb{R}^d$  is the  $d$ -dimensional embedding of the  $i$ -th unlabeled peptide.

We cluster these peptide embeddings into  $K$  clusters<sup>1</sup> using the K-Means algorithm [22]. The initial cluster centers are denoted as  $\mathbf{C} = \{\mathbf{c}_1, \mathbf{c}_2, \dots, \mathbf{c}_K\} \in \mathbb{R}^{K \times d}$ . The pairwise distance  $V_{ij}$  between the  $i$ -th peptide embedding  $\mathbf{z}_i^l$  and the  $j$ -th cluster center  $\mathbf{c}_j$  is computed as:

$$V_{ij} = \left\| \mathbf{z}_i^l - \mathbf{c}_j \right\|_2, \quad \forall i \in \{1, 2, \dots, |\mathcal{N}_{\text{unlabel}}|\}, \quad (10)$$

$$\forall j \in \{1, 2, \dots, K\},$$

where  $V_{ij}$  denotes the Euclidean distance between  $\mathbf{z}_i^l$  and  $\mathbf{c}_j$ . Then, the distances are then converted into probabilities using a softmax function:

$$p_{ij} = \frac{\exp(-V_{ij})}{\sum_{n=1}^K \exp(-V_{in})}. \quad (11)$$

Finally, the pseudo-label  $\hat{y}_i$  for  $i$ -th unlabeled peptide is assigned to the class with the highest probability:

$$\hat{y}_i = \arg \max_j p_{ij}. \quad (12)$$

Moreover, to emphasize high-confidence predictions, we define the associated confidence score for each unlabeled peptide. In details, for  $i$ -th unlabeled peptide, the confidence score  $s_i$  is calculated as

$$s_i = \max_j p_{ij}, \quad (13)$$

which can reflect the model's certainty in its prediction. We then construct the confident sets for the unlabeled peptides based on their pseudo labels and confidence scores as follows:

$$\mathcal{N}_c^{\text{pos}} = \{i \mid \hat{y}_i = 1, s_i > \tau\},$$

$$\mathcal{N}_c^{\text{neg}} = \{j \mid \hat{y}_j = 0, s_j > \tau\}, \quad (14)$$

$$\forall i, j \in \{1, 2, \dots, |\mathcal{N}_{\text{unlabel}}|\},$$

where  $\mathcal{N}_c^{\text{pos}}$  represents the confident set of peptides with the pseudo label  $\hat{y} = 1$ , and  $\mathcal{N}_c^{\text{neg}}$  represents the confident set of peptides with the pseudo label  $\hat{y} = 0$ . Here,  $\tau$  is a predefined threshold value, which is set to 0.5 for convenience. These confident sets form the foundation for further training and refinement in the AMP classification task.

For further adapting to evolving embedding distributions, the cluster centers are updated based on mean embeddings of

<sup>1</sup>  $K = 2$ , representing AMP and non-AMP classes

the confident samples assigned to each cluster. For cluster  $j$ , the new cluster center  $\hat{\mathbf{c}}_j$  is computed as:

$$\hat{\mathbf{c}}_j = \frac{1}{|\mathcal{N}_c^j|} \sum_{i \in \mathcal{N}_c^j} \mathbf{z}_i^l, \quad (15)$$

$$\forall j \in \{\text{pos, neg}\},$$

where  $\mathcal{N}_c^j$  is the set of confident samples assigned to cluster  $j$ ,  $|\mathcal{N}_c^j|$  is the size of  $\mathcal{N}_c^j$ .

Next, to mitigate the class imbalance inherent in AMP and non-AMP data, class-specific weights are introduced, which are denoted as  $\omega_{cl}^{\text{pos}}$  for AMP data and  $\omega_{cl}^{\text{neg}}$  for non-AMP data. Specifically,  $\omega_{pl}^{\text{pos}}$  is calculated as:

$$\omega_{pl}^{\text{pos}} = 1 - \frac{|\mathcal{N}_c^{\text{pos}}|}{|\mathcal{N}_c^{\text{pos}}| + |\mathcal{N}_c^{\text{neg}}|}, \quad (16)$$

similarly,  $\omega_{pl}^{\text{neg}}$  is calculated by:

$$\omega_{pl}^{\text{neg}} = 1 - \frac{|\mathcal{N}_c^{\text{neg}}|}{|\mathcal{N}_c^{\text{pos}}| + |\mathcal{N}_c^{\text{neg}}|}. \quad (17)$$

The positive pseudo label loss,  $\mathcal{L}_{pl}^{\text{pos}}$ , is calculated as:

$$\mathcal{L}_{pl}^{\text{pos}} = \omega_{pl}^{\text{pos}} \frac{1}{|\mathcal{N}_c^{\text{pos}}|} \sum_{i \in \mathcal{N}_c^{\text{pos}}} -\log(p_{i, \hat{y}=1}), \quad (18)$$

where  $p_{i, \hat{y}=1}$  denotes the predicted probability of the  $i$ -th unlabeled peptides in  $\mathcal{N}_c^{\text{pos}}$ . Conversely, the negative pseudo label loss,  $\mathcal{L}_{pl}^{\text{neg}}$ , is expressed as:

$$\mathcal{L}_{pl}^{\text{neg}} = \omega_{pl}^{\text{neg}} \frac{1}{|\mathcal{N}_c^{\text{neg}}|} \sum_{j \in \mathcal{N}_c^{\text{neg}}} -\log(p_{j, \hat{y}=0}), \quad (19)$$

where  $p_{j, \hat{y}=0}$  is the predicted probability of the  $j$ -th unlabeled peptides in  $\mathcal{N}_c^{\text{neg}}$ .

Furthermore, a soft-label refinement loss is introduced using Kullback-Leibler (KL) divergence to refine pseudo-labels and maintain consistency across different layers of Graph Encoder. The soft-label refinement loss is defined as:

$$\mathcal{L}_{\text{soft}} = \alpha \frac{1}{|\mathcal{N}_c|} \sum_{i=1}^{|\mathcal{N}_c|} \sum_{j=1}^K p_{ij} \log \left( \frac{p_{ij}}{\hat{p}_{ij}} \right), \quad (20)$$

where  $\mathcal{N}_c = \mathcal{N}_c^{\text{pos}} \cup \mathcal{N}_c^{\text{neg}}$ ,  $|\mathcal{N}_c|$  is the size of  $\mathcal{N}_c$ ,  $p_{ij}$  is the probability of the  $i$ -th unlabeled peptides belonging to class  $j$  from layer  $l$ ,  $\hat{p}_{ij}$  is the predicted probability of the  $i$ -th unlabeled peptides belonging to class  $j$  from layer  $L$ , and  $\alpha = 1 - \bar{c}$  is a dynamic weighting factor influenced by the mean confidence, which is defined as

$$\bar{c} = \frac{1}{|\mathcal{N}_c|} \sum_{i=1}^{|\mathcal{N}_c|} \max_j p_{ij}. \quad (21)$$

The overall Weight-enhanced Pseudo-label loss,  $\mathcal{L}_{pl}$ , integrates the above three components:

$$\mathcal{L}_{pl} = \mathcal{L}_{pl}^{\text{pos}} + \mathcal{L}_{pl}^{\text{neg}} + \mathcal{L}_{\text{soft}}. \quad (22)$$

This composite loss ensures balanced pseudo-label learning, aligning the model's predictions with true distributions while addressing class imbalances and refining pseudo-label accuracy.

## 2.5 Learning Framework

To ensure effective learning from supervised data, we minimize the expected error for labeled data using a classification loss. Assuming the Graph encoder has  $L$  message passing layers, we extract the embeddings of the final layer, where  $\mathbf{Z}^L = [\mathbf{z}_1^L, \mathbf{z}_2^L, \dots, \mathbf{z}_{|\mathcal{N}_{\text{label}}|}^L]^T \in \mathbb{R}^{|\mathcal{N}_{\text{label}}| \times d}$  for  $|\mathcal{N}_{\text{label}}|$  labeled peptide graphs, where  $\mathbf{z}_i^L \in \mathbb{R}^d$  is the  $d$ -dimensional embedding of the  $i$ -th peptides, and the corresponding label vector  $\mathbf{y} = [y_1, y_2, \dots, y_{|\mathcal{N}_{\text{label}}|}]$ . The classification loss is defined as:

$$\mathcal{L}_{\text{cf}} = \frac{1}{|\mathcal{N}_{\text{label}}|} \sum_{i=1}^{|\mathcal{N}_{\text{label}}|} \text{CE}(\text{MLP}(\mathbf{z}_i^L), y_i), \quad (23)$$

where  $\text{MLP}(\cdot)$  is a multi-layer perceptron that maps the protein embedding  $\mathbf{z}_i^L$  to the predicted label space, and  $\text{CE}(\cdot, \cdot)$  represents the cross-entropy loss function.

Finally, the overall training objective of SGAC combines the classification loss  $\mathcal{L}_{\text{cf}}$ , the Weight-enhanced Contrastive Learning loss  $\mathcal{L}_{\text{cl}}$  and the Weight-enhanced Pseudo-label loss  $\mathcal{L}_{\text{pl}}$ , which is formulated as follows:

$$\mathcal{L} = \mathcal{L}_{\text{cf}} + \lambda \mathcal{L}_{\text{cl}} + \gamma \mathcal{L}_{\text{pl}}, \quad (24)$$

where  $\lambda$  and  $\gamma$  are hyperparameters that balance the ratio of the Weight-enhanced Contrastive Learning loss and the Weight-enhanced Pseudo-label loss relative to the classification loss. These components enable our SGAC to effectively integrate labeled data, structural information, and pseudo-labeled samples, ensuring robust and balanced learning for AMP and non-AMP classification.

## 2.6 AMP Prediction

In the final stage of our framework, we predict whether a given peptide sequence belongs to the AMP class or the non-AMP class based on the learned graph representations. The AMP prediction process leverages the comprehensive features captured by the Graph Encoder, as well as the refinements provided by Weight-enhanced Contrastive Learning and Weight-enhanced Pseudo-label Distillation.

Given the graph-level representation  $\mathbf{z}_i$  of  $i$ -th peptide graph generated by the Graph Encoder, we employ a Multi-Layer Perceptron (MLP) for classification. Specifically, the prediction probability  $p_{ij}$  is computed as:

$$p_{ij} = \text{softmax}(\text{MLP}(\mathbf{z}_i)), \quad (25)$$

where the MLP  $(\cdot)$  maps the graph representation  $\mathbf{z}_i$  to a probability distribution over the AMP and non-AMP classes.

The final classification decision for  $i$ -th peptide is determined by:

$$\bar{y}_i = \arg \max_j p_{ij}, \quad (26)$$

where  $\bar{y}_i$  is the predicted label for the  $i$ -th peptide.

## 3. Experiments

In this section, we conduct extensive experiments to verify the effectiveness of SGAC in AMP and non-AMP classification task.

### 3.1 Experimental settings

**Dataset.** The AMP data was sourced from the DRAMP database [33], which provides detailed annotations of

**Table 1.** Statistics of the AMP and non-AMP datasets, which presents the number of graphs, average nodes, and average edges for the complete dataset, as well as for AMPs and non-AMPs separately.

Datasets	Graphs	Avg. Nodes	Avg. Edges	Classes
AMPs & non-AMPs	65,971	38.8	195.8	2
AMPs	7,697	23.1	118.6	2
non-AMPs	58,274	40.9	206.1	2

antimicrobial peptides, while the non-AMP data was obtained from [34]. To ensure consistency, both AMP and non-AMP sequences were filtered to include only peptides with lengths ranging from 10 to 50 amino acids [26, 47]. Following the graph construction methodology described in Section 2.1, these amino acid sequences are transformed into graphs using their predicted 3D structures derived from amino acid sequences. The statistics of the processed datasets are presented in Table 1. Additionally, we adopt a standard random stratified split of the dataset into training (70%), testing (10%), and validation (20%) sets.

**Baselines.** To validate the effectiveness of SGAC, we compare three categories of methods: (1) five sequence-based methods, including BERT [14], Attention [43], LSTM [23], Random Forest [5], and Diff-AMP [48]; (2) three general graph neural networks (GNNs), namely GCN [28], GIN [56] and GraphSAGE [20]; and three recent GNNs-based AMP prediction methods, namely sAMPpred [58], MP-BERT [2] and PGAT [21].

**Evaluation metrics.** To comprehensively evaluate the performance of SGAC, we employ two widely used metrics for imbalanced classification tasks, F1 score and Matthews Correlation Coefficient (MCC) [11, 15], which provide complementary insights into model performance under class imbalance.

- **F1 score** is the harmonic mean of precision and recall, which evaluates the balance between false positives and false negatives. It is particularly effective in imbalanced datasets and is computed as follows:

$$\text{Precision} = \frac{\text{True Positive}}{\text{True Positive} + \text{False Positive}}, \quad (27)$$

$$\text{Recall} = \frac{\text{True Positive}}{\text{True Positive} + \text{False Negative}}, \quad (28)$$

$$\text{F1 Score} = \frac{2 \times \text{Precision} \times \text{Recall}}{\text{Precision} + \text{Recall}}. \quad (29)$$

A higher F1 score indicates better overall model performance.

- **Matthews Correlation Coefficient (MCC)** is a robust metric that considers all four outcomes of the confusion matrix: true positives (TP), true negatives (TN), false positives (FP), and false negatives (FN). This balanced formulation makes it particularly suitable for evaluating models on imbalanced datasets. It is defined as:

$$\text{MCC} = \frac{(TP \times TN) - (FP \times FN)}{\sqrt{(TP + FP)(TP + FN)(TN + FP)(TN + FN)}}. \quad (30)$$

MCC ranges from  $-1$  to  $+1$ , where  $+1$  indicates perfect prediction,  $0$  corresponds to random guessing, and  $-1$

**Table 2.** Performance comparison among baselines and SGAC across different AMP length intervals and the full dataset. **Bold** results indicate the best performance.

Type	Methods	10–20		20–40		40–50		Full	
		F1	MCC	F1	MCC	F1	MCC	F1	MCC
Sequential	BERT	73.43 ± 0.22	56.91 ± 0.12	72.54 ± 0.37	55.58 ± 0.28	70.41 ± 0.42	52.12 ± 0.18	71.33 ± 0.48	54.44 ± 0.36
	Diff-AMP	61.95 ± 1.02	38.31 ± 0.79	60.22 ± 0.76	34.17 ± 1.33	58.94 ± 0.65	33.30 ± 0.56	61.08 ± 0.75	37.33 ± 0.89
	LSTM	84.76 ± 0.92	69.85 ± 0.88	82.60 ± 1.06	65.30 ± 0.72	79.96 ± 1.32	60.01 ± 0.67	82.09 ± 0.90	66.44 ± 0.75
	Attention	83.09 ± 0.77	66.27 ± 0.65	80.61 ± 1.21	63.42 ± 0.85	77.17 ± 1.09	59.09 ± 0.78	81.11 ± 0.89	65.19 ± 0.71
	Random Forest	92.21	85.03	90.64	82.45	87.01	76.03	87.97	78.08
General Graph	GCN	92.82 ± 0.55	85.08 ± 0.32	84.21 ± 0.83	73.08 ± 0.48	78.98 ± 0.94	61.03 ± 0.61	88.19 ± 0.68	81.22 ± 0.56
	GraphSAGE	93.01 ± 0.76	86.11 ± 0.42	85.33 ± 0.73	75.12 ± 0.55	80.17 ± 0.67	63.38 ± 0.54	91.15 ± 0.71	84.08 ± 0.48
	GIN	93.72 ± 0.64	86.39 ± 0.53	86.77 ± 0.49	76.39 ± 0.39	83.30 ± 0.82	65.18 ± 0.76	92.12 ± 0.74	85.33 ± 0.59
Graph-based AMP	sAMPpred	93.03 ± 0.55	86.55 ± 0.41	90.78 ± 0.69	83.46 ± 0.48	87.12 ± 0.98	79.44 ± 0.80	91.01 ± 0.73	82.39 ± 0.57
	MP-BERT	92.66 ± 0.66	87.09 ± 0.50	91.00 ± 0.43	84.88 ± 0.61	89.36 ± 0.83	82.98 ± 0.73	91.53 ± 0.55	85.19 ± 0.63
	PGAT	93.91 ± 0.43	87.33 ± 0.32	91.33 ± 0.56	84.67 ± 0.44	89.01 ± 0.69	81.72 ± 0.52	93.04 ± 0.49	86.98 ± 0.48
	SGAC	<b>95.31 ± 0.59</b>	<b>94.68 ± 0.48</b>	<b>93.63 ± 0.70</b>	<b>92.52 ± 0.52</b>	<b>91.25 ± 0.81</b>	<b>90.12 ± 0.49</b>	<b>94.83 ± 0.77</b>	<b>93.02 ± 0.56</b>

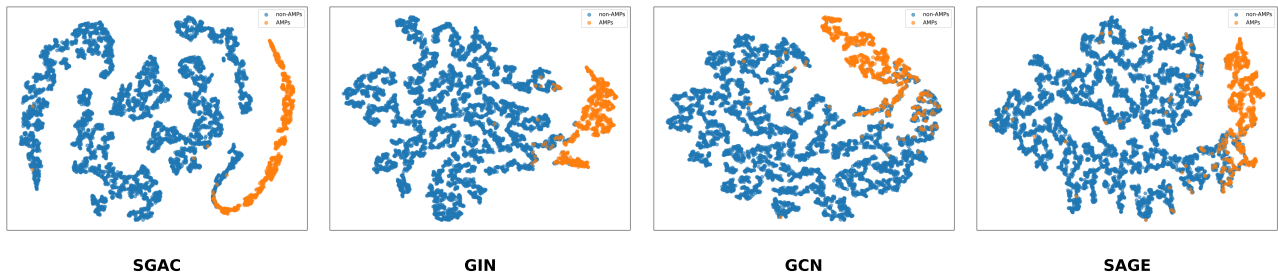


**Fig. 2.** AMP and non-AMP classification visualization using different models.

**Table 3.** The performance of SGAC with different GNN architectures on the full dataset. **Bold** results indicate the best performance.

Method	F1	MCC
SGAC w GCN	92.45 ± 0.47	91.31 ± 0.39
SGAC w GraphSAGE	93.75 ± 0.64	92.58 ± 0.43
<b>SGAC w GIN</b>	<b>94.83 ± 0.77</b>	<b>93.02 ± 0.56</b>

indicates total disagreement. Higher MCC values reflect more reliable performance under imbalance.

**Implementation details.** Random Forest is implemented using scikit-learn<sup>2</sup>, while all other models, including SGAC and other baselines are implemented using PyTorch<sup>3</sup>. For SGAC, we use GIN [56] as the backbone for the Graph Encoder introduced in Section 2.2, incorporating a mean-pooling layer as the readout function. All experiments for SGAC and baselines are conducted on NVIDIA A100 GPUs to ensure a fair comparison, where the learning rate of Adam optimizer is set to  $10^{-4}$ , hidden embedding dimension 256, weight decay  $10^{-12}$ , and GNN layers 4. For all methods, we re-trained the models from scratch using the same data splitting strategy, and the performance of each method was evaluated on all samples and reported as the average over five independent runs.

### 3.2 Performance comparisons

We present the results of the proposed SGAC and all baselines in Table 2. We can observe that (1) Random

Forest demonstrates the highest performance among sequence-based methods, indicating its strong capability in extracting informative features from amino acid sequences. Nevertheless, it remains inferior to graph-based models, which emphasize the limitations of sequence-based methods in capturing the structural and relational information inherent in proteins. (2) General graph neural networks (GNNs) outperform sequence-based approaches on most cases, highlighting the advantage of modeling peptides as graph structures. Among these models, GIN achieves the best results, surpassing both GCN and GraphSAGE, which demonstrates the ability of GNNs to effectively capture the structural and relational dependencies within peptide graphs. (3) Recent graph-based AMP prediction methods, such as sAMPpred, MP-BERT, and PGAT, further improve performance compared with general GNNs. Their superior results can be attributed to the integration of peptide-specific structural priors and spatial constraints, enabling these models to better capture biologically meaningful geometric relationships that drive antimicrobial activity. (4) SGAC outperforms all baselines across all evaluation settings and peptide length intervals, achieving the highest F1 and MCC scores in every case. This consistent superiority underscores the effectiveness of SGAC’s design, which leverages spatial structural information and mitigates class imbalance through weighted-enhanced contrastive learning and pseudo-label refinement. Specifically, the Weight-enhanced Contrastive Learning module strengthens AMP-specific structural discrimination under imbalanced conditions, while the Weight-enhanced Pseudo-label Distillation module iteratively refines pseudo labels to preserve semantic consistency and improve minority-class representation. Together, these modules enable SGAC to achieve robust, balanced, and discriminative AMP classification across diverse peptide lengths and imbalanced datasets.

<sup>2</sup> <https://scikit-learn.org/>

<sup>3</sup> <https://pytorch.org/>

**Table 4.** The results of ablation studies. **Bold** results indicate the best performance per column.

Method	F1	MCC
SGAC w/o cf	$74.17 \pm 0.41$	$72.19 \pm 0.33$
SGAC w/o pl	$93.87 \pm 0.47$	$91.19 \pm 0.29$
SGAC w/o cl	$93.74 \pm 0.38$	$91.38 \pm 0.31$
SGAC w/o all	$92.12 \pm 0.74$	$85.33 \pm 0.59$
SGAC	<b><math>94.83 \pm 0.77</math></b>	<b><math>93.02 \pm 0.56</math></b>

We further evaluate the flexibility of the proposed SGAC by replacing different GNN architectures as the backbone of the Graph Encoder. Specifically, GIN is replaced with GCN and GraphSAGE, and the corresponding performance results are presented in Table 3. The results demonstrate that SGAC w/ GIN consistently achieves the best performance across all metrics. This superior performance underscores GIN’s strong representational capacity, enabling it to effectively capture the structural and relational characteristics of graph-structured data. This phenomenon also justifies using GIN as the backbone of Graph Encoder to enhance the proposed SGAC performance. Additionally, the visualization results among SGAC and general GNNs are shown in Figure 2, the embeddings produced by SGAC exhibit a clear separation between AMPs and non-AMPs, indicating that the model effectively learns discriminative representations. In contrast, the embeddings from general GNNs show a less defined boundary, further highlighting the contribution of the learning modules proposed in SGAC.

### 3.3 Ablation study

We conduct ablation studies to evaluate the contribution of each component in the proposed SGAC: (1) SGAC w/o cf: removes the classification loss  $\mathcal{L}_{cf}$ ; (2) SGAC w/o pl: removes the Weight-enhanced Pseudo-label Distillation loss  $\mathcal{L}_{pl}$ ; (3) SGAC w/o cl: removes the Weight-enhanced Contrastive Learning loss  $\mathcal{L}_{cl}$ ; (4) SGAC w/o all: removes all auxiliary objectives, retaining only the encoder and classifier.

Experimental results are shown in Table 4. From the table, we find that (1) SGAC w/o cf shows lower performance compared to SGAC, showing that  $\mathcal{L}_{cf}$  is crucial in leveraging labeled data effectively. This result also indicates that  $\mathcal{L}_{cf}$  is crucial in guiding the model to learn meaningful and robust graph representations. (2) SGAC w/o pl exhibits a noticeable decline in performance compared to SGAC, confirming the critical role of the Weight-enhanced Pseudo-label Distillation module. This component refines pseudo labels for unlabeled or uncertain peptides according to prediction confidence and class distribution, allowing the model to leverage high-confidence samples while maintaining balanced learning between AMPs and non-AMPs. By exposing the model to a broader and more informative sample space, this mechanism improves generalization under severe class imbalance. (3) SGAC also consistently outperforms SGAC w/o cl across all metrics, demonstrating the effectiveness of the Weight-enhanced Contrastive Learning module. By assigning adaptive weights to sample pairs based on class frequency, this module enhances intra-class cohesion and inter-class separation, ensuring that minority AMP samples are adequately represented in the embedding space. This adaptive weighting effectively mitigates bias toward the dominant non-AMP class and strengthens the discriminative power of the learned representations. (4) SGAC w/o all exhibits the

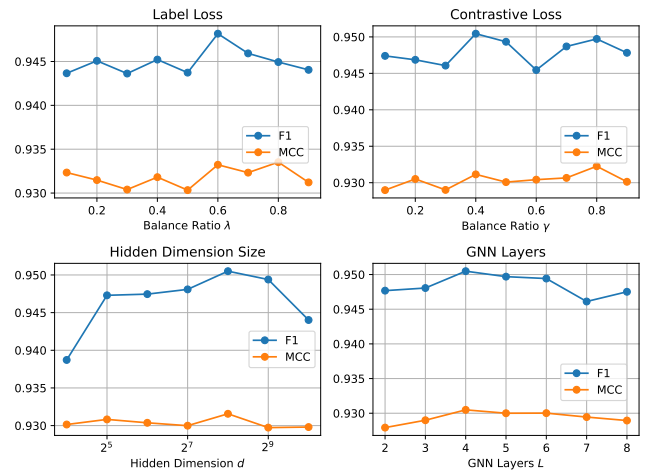


**Fig. 3.** Hyper-parameter sensitivity analysis of  $\lambda$ ,  $\gamma$ , Hidden dimension size  $d$  and GNN layers  $L$ .

lowest performance, underscoring their synergistic importance. Without the Weight-enhanced Contrastive Learning and Pseudo-label Distillation components, the model fails to balance class distributions or capture subtle structural distinctions between AMPs and non-AMPs. Consequently, its learned representations become biased and less discriminative, leading to substantial drops in both F1 and MCC.

### 3.4 Sensitivity Analysis

We study the sensitivity analysis of SGAC with respect to the impact of its hyperparameters: balance ratio  $\lambda$  and  $\gamma$ , hidden dimension size  $d$ , and GNN layers  $L$ , which plays a crucial role in the performance of SGAC. Especially,  $\lambda$  and  $\gamma$  control the relative contributions of  $\mathcal{L}_{cl}$  and  $\mathcal{L}_{pl}$  to the overall objective, ensuring practical trade-offs between classification, contrastive learning, and pseudo-label distillation;  $d$  determines the dimension of the learned graph representations, which directly impacts the model’s capacity to capture structural and relational information;  $L$  governs the depth of message passing in the GNNs, which influences the ability to aggregate information from neighbors and model higher-order relationships in the graph.

Figure 3 illustrates how  $\lambda$ ,  $\gamma$ ,  $d$  and  $L$  affects the performance of SGAC. We vary  $\lambda$  and  $\gamma$  within the range of  $\{0.1, 0.2, 0.3, 0.4, 0.5, 0.6, 0.7, 0.8, 0.9\}$ ,  $d$  in  $\{2^4, 2^5, 2^6, 2^7, 2^8, 2^9, 2^{10}\}$ , and  $L$  in  $\{2, 3, 4, 5, 6, 7, 8\}$ . From the results, we observe that: (1) The performance of SGAC in Figure 3 generally stabilizes across a wide range of  $\lambda$  values and  $\gamma$  values. The slight variations in the F1 score indicate a potential trade-off among the contributions of  $\mathcal{L}_{cf}$ ,  $\mathcal{L}_{cl}$  and  $\mathcal{L}_{pl}$ . SGAC achieves optimal performance around  $\lambda = 0.6$  and  $\gamma = 0.4$ , which is chosen as the default setting. (2) The performance of SGAC improves, as  $d$  increases from  $2^4$  to  $2^8$ , peaking at  $d = 2^8$ . Then, the F1 score slightly declines, while AUC and PR-AUC plateau. This indicates that larger dimensions may introduce overfitting or unnecessary complexity without yielding substantial performance improvements. Therefore,  $d = 2^8$  is selected as the optimal hidden dimension size. (3) The performance of SGAC improves and then keeps stable as  $L$  increases from 2 to 6, demonstrating that deeper architectures effectively capture structural information of protein graphs.

**Table 5.** Statistics of the dataset used in the case study, showing the number of graphs, average nodes, and average edges for AMPs, non-AMPs, and their combined dataset.

Datasets	Graphs	Avg. Nodes	Avg. Edges	Classes
AMPs & non-AMPs	78	23.1	51.7	2
AMPs	55	23.3	52.3	2
non-AMPs	23	22.5	50.1	2

**Table 6.** Analysis of Misclassified Samples and Closest Structural Matches.

Misclassified ID	True → Pred	Closest Match ID	RMSD
424290	1 → 0	2906279	1.2891
425545	1 → 0	2906672	0.6041
426383	0 → 1	DRAMP04626	0.8319
434399	0 → 1	DRAMP35858	0.6786
439751	0 → 1	DRAMP33369	0.7193

However, when  $L > 6$ , the model performance slightly drops due to over-smoothing.  $L = 4$  is selected as the default value to balance performance and computational efficiency.

### 3.5 Case study

To test the practicality of SGAC, we conducted a case study utilizing the potential antimicrobial peptide data synthesized in [42]. They utilized MetaProdigal to identify 444,000 small open reading frames (smORFs) from 1,773 human microbiome metagenomes. Subsequently, they utilized AmPEP, a random forest classifier, to predict the antimicrobial activity of these smORFs, resulting in 323 smORF-encoded candidate antimicrobial peptides (SEPs). Through a series of selection criteria, they selected 78 high-priority antimicrobial peptides for synthesis and experimental validation. The vitro experiments indicate that 70.5% (55/78) of the synthesized SEPs exhibited antimicrobial activity against at least one pathogen. Following the preprocessing methodology detailed in Section 2.1, graphs are constructed for these peptides, where the statistics of these graphs are summarized in Table 5. These peptide graphs are then input into the trained SGAC model for inference. The experimental results show that SGAC accurately classified 40 of the true AMPs and 5 of the non-AMPs.

To better understand this phenomenon, we investigate model behavior on these misclassified samples. Specifically, we randomly select five misclassified peptides and evaluate their structural similarity to samples from the training set using the Root Mean Square Deviation (RMSD) between  $C_\alpha$  coordinates. We identify the closest structural match from the training data for each misclassified sample. The results are presented in Table 6, including the misclassified sample ID, the misprediction direction, the matched sample ID, and the corresponding RMSD score. These findings suggest that peptides with highly similar spatial structures ( $\text{RMSD} < 1.5$ ) may still exhibit distinct biological functions, leading to misclassification. Furthermore, high structural similarity can result in intrinsic representational overlap between AMP and non-AMP samples, making it difficult for the model to distinguish them with high confidence. In future work, we plan to incorporate additional biological properties, such as physicochemical characteristics, sequence motifs, and functional annotations, to enhance the robustness and interpretability of peptide classification models.

## Conclusion

In this study, we proposed SGAC, a Spatial GNN-based framework for distinguishing antimicrobial peptides (AMPs) from non-AMPs by leveraging peptide three-dimensional structural information. SGAC constructs compact  $C_\alpha$ -based peptide graphs predicted by OmegaFold and integrates two key modules, Weight-enhanced Contrastive Learning and Weight-enhanced Pseudo-label Distillation, to address the challenges of class imbalance and limited labeled data. Through adaptive weighting and iterative pseudo-label refinement, SGAC achieves balanced, discriminative, and consistent representation learning. Extensive experiments on public AMP datasets demonstrate that SGAC outperforms both sequence-based and graph-based baselines, achieving state-of-the-art performance. Ablation and sensitivity analyses further verify the contributions of each component, and a biosynthetic case study highlights SGAC’s potential in accelerating peptide discovery and supporting antibiotic research. In future work, we plan to incorporate additional biological properties, such as physicochemical characteristics, sequence motifs, and functional annotations, to enhance the robustness and interpretability of peptide classification models.

## References

1. Benita S Arakal, David E Whitworth, Philip E James, Richard Rowlands, Neethu PT Madhusoodanan, Malvika R Baijoo, and Paul G Livingstone. In silico and in vitro analyses reveal promising antimicrobial peptides from myxobacteria. *Probiotics and Antimicrobial Proteins*, 15(1):202–214, 2023.
2. Srivathsan Badrinarayanan, Chakradhar Guntuboina, Parisa Mollaei, and Amir Barati Farimani. Multi-peptide: multimodality leveraged language-graph learning of peptide properties. *Journal of Chemical Information and Modeling*, 65(1):83–91, 2024.
3. Pratiti Bhadra, Jielu Yan, Jinyan Li, Simon Fong, and Shirley WI Siu. Ampep: Sequence-based prediction of antimicrobial peptides using distribution patterns of amino acid properties and random forest. *Scientific reports*, 8(1):1697, 2018.
4. Thomas CG Bosch and Michael Zasloff. Antimicrobial peptides—or how our ancestors learned to control the microbiome. *MBio*, 12(5):10–1128, 2021.
5. Leo Breiman. Random forests. *Machine learning*, 45:5–32, 2001.
6. Cezara Bucataru and Corina Ciobanu. Antimicrobial peptides: Opportunities and challenges in overcoming resistance. *Microbiological Research*, page 127822, 2024.
7. Nanjun Chen, Jixiang Yu, Liu Zhe, Fuzhou Wang, Xiangtao Li, and Ka-Chun Wong. Tp-lmmsg: a peptide prediction graph neural network incorporating flexible amino acid property representation. *Briefings in Bioinformatics*, 25(4):bbae308, 2024.
8. Xiaoru Chen, Yingxu Wang, Jinyuan Fang, Zaiqiao Meng, and Shangsong Liang. Heterogeneous graph contrastive learning with metapath-based augmentations. *IEEE Transactions on Emerging Topics in Computational Intelligence*, 2023.
9. Yu Chen, Xingpeng Jiang, and Weizhong Zhao. Amppred-dlff: prediction of amps based on deep learning and multi-view features fusion. In *2024 IEEE International Conference on Bioinformatics and Biomedicine (BIBM)*, 2024.

pages 891–896. IEEE, 2024.

10. Zixin Chen, Chengming Ji, Wenwen Xu, Jianfeng Gao, Ji Huang, Huanliang Xu, Guoliang Qian, and Junxian Huang. Uniamp: enhancing amp prediction using deep neural networks with inferred information of peptides. *BMC bioinformatics*, 26(1):10, 2025.
11. Davide Chicco and Giuseppe Jurman. The matthews correlation coefficient (mcc) should replace the roc auc as the standard metric for assessing binary classification. *BioData Mining*, 16(1):4, 2023.
12. Juan-Pablo Couso and Pedro Patraquim. Classification and function of small open reading frames. *Nature reviews Molecular cell biology*, 18(9):575–589, 2017.
13. Meili Cui, Mengyue Wang, Xia Liu, Haoyan Sun, Zhenghua Su, Yu Zheng, Yanbing Shen, and Min Wang. Mining and characterization of novel antimicrobial peptides from the large-scale microbiome of shanxi aged vinegar based on metagenomics, molecular dynamics simulations and mechanism validation. *Food Chemistry*, 460:140646, 2024.
14. Jacob Devlin. Bert: Pre-training of deep bidirectional transformers for language understanding. *arXiv preprint arXiv:1810.04805*, 2018.
15. Ramatoulaye Diallo, Codjo Edalo, and O Olawale Awe. Machine learning evaluation of imbalanced health data: a comparative analysis of balanced accuracy, mcc, and f1 score. In *Practical Statistical Learning and Data Science Methods: Case Studies from LISA 2020 Global Network, USA*, pages 283–312. Springer, 2024.
16. Matthew G Durrant and Ami S Bhatt. Automated prediction and annotation of small open reading frames in microbial genomes. *Cell host & microbe*, 29(1):121–131, 2021.
17. Fabiano C Fernandes, Marlon H Cardoso, Abel Gil-Ley, Lívia V Luchi, Maria GL da Silva, Maria LR Macedo, Cesar de la Fuente-Nunez, and Octavio L Franco. Geometric deep learning as a potential tool for antimicrobial peptide prediction. *Frontiers in Bioinformatics*, 3:1216362, 2023.
18. Raúl Fernández-Díaz, Rodrigo Cossío-Pérez, Clement Agoni, Hoang Thanh Lam, Vanessa Lopez, and Denis C Shields. Autopeptideml: a study on how to build more trustworthy peptide bioactivity predictors. *Bioinformatics*, 40(9):btae555, 2024.
19. Limin Fu, Beifang Niu, Zhengwei Zhu, Sitao Wu, and Weizhong Li. Cd-hit: accelerated for clustering the next-generation sequencing data. *Bioinformatics*, 28(23):3150–3152, 2012.
20. Will Hamilton, Zhitao Ying, and Jure Leskovec. Inductive representation learning on large graphs. *Advances in neural information processing systems*, 30, 2017.
21. Yuelei Hao, Xuyang Liu, Haohao Fu, Xueguang Shao, and Wensheng Cai. Pgat-abpp: harnessing protein language models and graph attention networks for antibacterial peptide identification with remarkable accuracy. *Bioinformatics*, 40(8):btae497, 2024.
22. John A Hartigan, Manchek A Wong, et al. A k-means clustering algorithm. *Applied statistics*, 28(1):100–108, 1979.
23. S Hochreiter. Long short-term memory. *Neural Computation MIT-Press*, 1997.
24. Junjie Huang, Yanchao Xu, Yunfan Xue, Yue Huang, Xu Li, Xiaohui Chen, Yao Xu, Dongxiang Zhang, Peng Zhang, Junbo Zhao, et al. Identification of potent antimicrobial peptides via a machine-learning pipeline that mines the entire space of peptide sequences. *Nature Biomedical Engineering*, 7(6):797–810, 2023.
25. Doug Hyatt, Philip F LoCascio, Loren J Hauser, and Edward C Uberbacher. Gene and translation initiation site prediction in metagenomic sequences. *Bioinformatics*, 28(17):2223–2230, 2012.
26. Kanchan Jha, Sriparna Saha, and Hiteshi Singh. Prediction of protein–protein interaction using graph neural networks. *Scientific Reports*, 12(1):8360, 2022.
27. John Jumper, Richard Evans, Alexander Pritzel, Tim Green, Michael Figurnov, Olaf Ronneberger, Kathryn Tunyasuvunakool, Russ Bates, Augustin Žídek, Anna Potapenko, et al. Highly accurate protein structure prediction with alphafold. *nature*, 596(7873):583–589, 2021.
28. Thomas N Kipf and Max Welling. Semi-supervised classification with graph convolutional networks. *arXiv preprint arXiv:1609.02907*, 2016.
29. Naveen Kumar, Prashant Bhagwat, Suren Singh, and Santhosh Pillai. A review on the diversity of antimicrobial peptides and genome mining strategies for their prediction. *Biochimie*, 2024.
30. Yujia Li, Daniel Tarlow, Marc Brockschmidt, and Richard Zemel. Gated graph sequence neural networks. *arXiv preprint arXiv:1511.05493*, 2015.
31. Ce Liu, Jun Wang, Zhiqiang Cai, Yingxu Wang, Huizhen Kuang, Kaihui Cheng, Liwei Zhang, Qingkun Su, Yining Tang, Fenglei Cao, et al. Dynamic pdb: A new dataset and a se (3) model extension by integrating dynamic behaviors and physical properties in protein structures. *arXiv preprint arXiv:2408.12413*, 2024.
32. Licheng Liu, Caiyun Wang, Mengyue Zhang, Zixuan Zhang, Yingying Wu, and Yixuan Zhang. An efficient evaluation system accelerates  $\alpha$ -helical antimicrobial peptide discovery and its application to global human genome mining. *Frontiers in Microbiology*, 13:870361, 2022.
33. Tianyue Ma, Yanchao Liu, Bingxin Yu, Xin Sun, Huiyuan Yao, Chen Hao, Jianhui Li, Maryam Nawaz, Xun Jiang, Xingzhen Lao, et al. Dramp 4.0: an open-access data repository dedicated to the clinical translation of antimicrobial peptides. *Nucleic Acids Research*, page gkae1046, 2024.
34. Yue Ma, Zhengyan Guo, Binbin Xia, Yuwei Zhang, Xiaolin Liu, Ying Yu, Na Tang, Xiaomei Tong, Min Wang, Xin Ye, et al. Identification of antimicrobial peptides from the human gut microbiome using deep learning. *Nature Biotechnology*, 40(6):921–931, 2022.
35. Maria Magana, Muthuirulan Pushpanathan, Ana L Santos, Leon Leanse, Michael Fernandez, Anastasios Ioannidis, Marc A Giulianotti, Yiorgos Apidianakis, Steven Bradfute, Andrew L Ferguson, et al. The value of antimicrobial peptides in the age of resistance. *The lancet infectious diseases*, 20(9):e216–e230, 2020.
36. Karla L Martínez-Mauricio, César R García-Jacas, and Greneter Cordoves-Delgado. Examining evolutionary scale modeling-derived different-dimensional embeddings in the antimicrobial peptide classification through a knime workflow. *Protein Science*, 33(4):e4928, 2024.
37. Md Abdus Salam, Md Yusuf Al-Amin, Moushumi Tabassoom Salam, Jogendra Singh Pawar, Naseem Akhter, Ali A Rabaan, and Mohammed AA Alquember. Antimicrobial resistance: a growing serious threat for global public health. In *Healthcare*, volume 11, page 1946. MDPI, 2023.
38. Célio Dias Santos-Junior, Shaojun Pan, Xing-Ming Zhao, and Luis Pedro Coelho. Macrel: antimicrobial peptide

screening in genomes and metagenomes. *PeerJ*, 8:e10555, 2020.

39. Célio Dias Santos-Júnior, Marcelo DT Torres, Yiqian Duan, Álvaro Rodríguez Del Río, Thomas SB Schmidt, Hui Chong, Anthony Fullam, Michael Kuhn, Chengkai Zhu, Amy Houseman, et al. Discovery of antimicrobial peptides in the global microbiome with machine learning. *Cell*, 2024.

40. Zehua Sun, Jing Xu, Yumeng Zhang, Yiwen Zhang, Zhikang Wang, Xiaoyu Wang, Shanshan Li, Yuming Guo, Hsin Hui Shen, and Jiangning Song. Multimodal geometric learning for antimicrobial peptide identification by leveraging alphafold2-predicted structures and surface features. *Briefings in Bioinformatics*, 26(3), 2025.

41. Garima Suneja, Sonam Nain, and Rakesh Sharma. Microbiome: A source of novel bioactive compounds and antimicrobial peptides. *Microbial Diversity in Ecosystem Sustainability and Biotechnological Applications: Volume 1. Microbial Diversity in Normal & Extreme Environments*, pages 615–630, 2019.

42. Marcelo DT Torres, Erin F Brooks, Angela Cesaro, Hila Sberro, Matthew O Gill, Cosmos Nicolaou, Ami S Bhatt, and Cesar de la Fuente-Nunez. Mining human microbiomes reveals an untapped source of peptide antibiotics. *Cell*, 187(19):5453–5467, 2024.

43. A Vaswani. Attention is all you need. *Advances in Neural Information Processing Systems*, 2017.

44. Boris Vishnepolsky, Maya Grigolava, Grigol Managadze, Andrei Gabrielian, Alex Rosenthal, Darrell E Hurt, Michael Tartakovsky, and Malak Pirtskhalava. Comparative analysis of machine learning algorithms on the microbial strain-specific amp prediction. *Briefings in Bioinformatics*, 23(4):bbac233, 2022.

45. Timothy R Walsh, Ana C Gales, Ramanan Laxminarayan, and Philippa C Dodd. Antimicrobial resistance: addressing a global threat to humanity, 2023.

46. Fangye Wang, Yingxu Wang, Dongsheng Li, Hansu Gu, Tun Lu, Peng Zhang, and Ning Gu. Cl4ctr: A contrastive learning framework for ctr prediction. In *Proceedings of the Sixteenth ACM International Conference on Web Search and Data Mining*, pages 805–813, 2023.

47. Guangshun Wang, Iosif I Vaisman, and Monique L van Hoek. Machine learning prediction of antimicrobial peptides. In *Computational peptide science: Methods and protocols*, pages 1–37. Springer, 2022.

48. Rui Wang, Tao Wang, Linlin Zhuo, Jinhang Wei, Xiangzheng Fu, Quan Zou, and Xiaojun Yao. Diffamp: tailored designed antimicrobial peptide framework with all-in-one generation, identification, prediction and optimization. *Briefings in Bioinformatics*, 25(2):bbae078, 2024.

49. Yingxu Wang, Mengzhu Wang, Zhichao Huang, Suyu Liu, and Nan Yin. Nested graph pseudo-label refinement for noisy label domain adaptation learning. *arXiv preprint arXiv:2508.00716*, 2025.

50. Yingxu Wang, Mengzhu Wang, Houcheng Su, Nan Yin, Quanming Yao, and James Kwok. Degree-conscious spiking graph for cross-domain adaptation. *arXiv preprint arXiv:2410.06883*, 2024.

51. Yingxu Wang, Nan Yin, Mingyan Xiao, Xinhao Yi, Siwei Liu, and Shangsong Liang. Dusego: Dual second-order equivariant graph ordinary differential equation. *ACM Transactions on Knowledge Discovery from Data*, 2024.

52. Yingxu Wang, Kunyu Zhang, Jiaxin Huang, Nan Yin, Siwei Liu, and Eran Segal. Protomol: enhancing molecular property prediction via prototype-guided multimodal learning. *Briefings in Bioinformatics*, 26(6):bbaf629, 2025.

53. Joseph L Watson, David Juergens, Nathaniel R Bennett, Brian L Trippe, Jason Yim, Helen E Eisenach, Woody Ahern, Andrew J Borst, Robert J Ragotte, Lukas F Milles, et al. Broadly applicable and accurate protein design by integrating structure prediction networks and diffusion generative models. *BioRxiv*, pages 2022–12, 2022.

54. Ruidong Wu, Fan Ding, Rui Wang, Rui Shen, Xiwen Zhang, Shitong Luo, Chenpeng Su, Zuofan Wu, Qi Xie, Bonnie Berger, et al. High-resolution de novo structure prediction from primary sequence. *BioRxiv*, pages 2022–07, 2022.

55. Chunming Xu, Aiping Han, Yuan Tian, and Shiguang Sun. Based on computer simulation and experimental verification: Mining and characterizing novel antimicrobial peptides from soil microbiome. *Food Chemistry*, page 142275, 2024.

56. Keyulu Xu, Weihua Hu, Jure Leskovec, and Stefanie Jegelka. How powerful are graph neural networks? *arXiv preprint arXiv:1810.00826*, 2018.

57. Jielu Yan, Pratiti Bhadra, Ang Li, Pooja Sethiya, Longguang Qin, Hio Kuan Tai, Koon Ho Wong, and Shirley WI Siu. Deep-ampep30: improve short antimicrobial peptides prediction with deep learning. *Molecular Therapy-Nucleic Acids*, 20:882–894, 2020.

58. Ke Yan, Hongwu Lv, Yichen Guo, Wei Peng, and Bin Liu. samppred-gat: prediction of antimicrobial peptide by graph attention network and predicted peptide structure. *Bioinformatics*, 39(1):btac715, 2023.

59. Bin Yang, Hongyan Yang, Jianlong Liang, Jiarou Chen, Chunhua Wang, Yuanyuan Wang, Jincai Wang, Wenhui Luo, Tao Deng, and Jiali Guo. A review on the screening methods for the discovery of natural antimicrobial peptides. *Journal of Pharmaceutical Analysis*, page 101046, 2024.

60. Tianjun Yao, Yingxu Wang, Kun Zhang, and Shangsong Liang. Improving the expressiveness of k-hop message-passing gnns by injecting contextualized substructure information. In *Proceedings of the 29th ACM SIGKDD Conference on Knowledge Discovery and Data Mining*, pages 3070–3081, 2023.

61. Jason Yim, Brian L Trippe, Valentin De Bortoli, Emile Mathieu, Arnaud Doucet, Regina Barzilay, and Tommi Jaakkola. Se (3) diffusion model with application to protein backbone generation. In *International Conference on Machine Learning*, pages 40001–40039. PMLR, 2023.

62. Yong Yu, Xiaosheng Si, Changhua Hu, and Jianxun Zhang. A review of recurrent neural networks: Lstm cells and network architectures. *Neural computation*, 31(7):1235–1270, 2019.